consisted of the CRE octamer in the contexts of the surrounding bases of the cAMP-unresponsive parathyroid hormone (PTH-8) and glucagon (GLU-8) genes and gave no transcriptional response to 8-bromo–cAMP, nor could they produce specific gel-shift patterns or compete for binding to a labeled "active CRE."
11. J. P. Hoeffler *et al.*, unpublished data.
12. D. Shalloway *et al.*, *Cell* **20**, 411 (1980).
13. W. H. Landschultz, P. F. Johnson, S. L. McKnight, *Science* **240**, 1759 (1988).
14. J. Garnier, D. J. Ogsthorpe, B. Robson, *J. Mol. Biol.* **120**, 97 (1978); J. Kyte and R. F. Doolittle, *ibid.* **157**, 105 (1982).
15. The sequence of CREB between residues 1 and 268 contains 25 glutamic acids and aspartic acids and 11 lysines and arginines. The corresponding sequence of c-Jun between residues 1 and 225 contains 22 glutamic acids and aspartic acids and 11 lysines and arginines.
16. P. S. Sigler, *Nature* **333**, 210 (1988); I. A. Hope, S. Mahadevan, K. Struhl, *ibid.* **333**, 635 (1988); J. Ma and M. Ptashne, *Cell* **48**, 847 (1987); G. Gill and M. Ptashne, *ibid.* **51**, 121 (1987).
17. Y.-S. Lin and M. R. Green, *Proc. Natl. Acad. Sci. U.S.A.* **85**, 3396 (1988); S. Hardy and T. Shenk, *ibid.* **85**, 4171 (1988).
18. Abbreviations for the amino acid residues are: A, Ala; C, Cys; D, Asp; E, Glu; F, Phe; G, Gly; H, His; I, Ile; K, Lys; L, Leu; M, Met; N, Asn; P, Pro; Q, Gln; R, Arg; S, Ser; T, Thr; V, Val; W, Trp; and Y, Tyr.
19. The authors thank G. Bruce for initial help with the λgt11 library, F. Traynor and M. LeSieur for expert experimental assistance, P. Sharp for information regarding the screening technique prior to publication, and J. Canniff for preparing the manuscript. Supported in part by NIH grants DK 25532 and DK 30457.

16 August 1988; accepted 7 November 1988

Newly Identified Brain Potassium Channels Gated by the Guanine Nucleotide Binding Protein G_o

A. M. J. VANDONGEN, J. CODINA, J. OLATE, R. MATTERA, R. JOHO, L. BIRNBAUMER, A. M. BROWN

Potassium channels in neurons are linked by guanine nucleotide binding (G) proteins to numerous neurotransmitter receptors. The ability of G_o, the predominant G protein in the brain, to stimulate potassium channels was tested in cell-free membrane patches of hippocampal pyramidal neurons. Four distinct types of potassium channels, which were otherwise quiescent, were activated by both isolated brain G_o and recombinant $G_o\alpha$. Hence brain G_o can couple diverse brain potassium channels to neurotransmitter receptors.

NEURONAL POTASSIUM CURRENTS are coupled by the G proteins G_i or G_o (*1–4*) to acetylcholine M2, adrenergic α_2, serotonin (5HT-1a), dopamine (D2), adenosine (A_1), γ-aminobutryic acid ($GABA_B$), opioid δ and μ, and somatostatin receptors (*1, 2*). Neuronal Ca^{2+} currents may be coupled similarly (*5*). Important evidence indicating this coupling is that the effects of the relevant neurotransmitter can be (i) mimicked by intracellular perfusion of guanosine-5′-*O*-(3-thiotriphosphate) (GTPγS); (ii) inhibited by intracellular perfusion of guanosine-5′-*O*-(2-thiodiphosphate) (GDPβS); or (iii) blocked by treatment of cells with pertussis toxin (PTX). Results with antibodies to G_o support this view (*1, 3–5*). The K^+ currents were in some cases identified as inwardly rectifying (*1, 2*) but the corresponding single channel K^+ currents have not been described; in fact there are only a few reports on neuronal single channel K^+ currents (*6–8*). We used single channel recordings to investigate the K^+ currents that are coupled to these receptors, and we tested whether G_o might, like G_k for atrial and clonal pituitary K^+ channels (*9*) or G_s for dihydropyridine-sensitive Ca^{2+} channels (*9*), gate or modulate neuronal K^+ channels directly.

In the first series of experiments (Fig. 1A), a highly purified preparation of preactivated G_o from bovine brain (*10, 11*) stimulated single channel K^+ currents in inside-out patches in a concentration-dependent manner. The major α subunit in this fraction was α_{39}; α_{41} and α_{40} were present at less than 5%, and α_z (*12*) may also have been present. We also tested another fraction that elutes before G_o and designated it "pre-G_o" (Fig. 2A, lane 1) (*11*). It contained mostly G_i with an α subunit of an apparent molecular mass of 41,000 daltons, another G protein with an α subunit of apparent molecular mass of 40,000 daltons, and a PTX-insensitive contaminant of about 55,000 daltons. The G proteins were activated with GTPγS (*11*), yielding activated G_o (G_o^*) and activated pre-G_o (pre-G_o^*); unbound nucleotide was removed by dialysis until the molar ratio of GTPγS to G protein was less than two. The activated G proteins were diluted at least by a factor of 100,000 in our bathing solutions. In some experiments, GTPγS at 100 μ*M* was tested to evaluate the effects of activating endogenous G proteins.

Our purified brain G_o could not be completely resolved into individual G proteins; therefore the reconstitution experiments infer, but do not prove, the identity of the putative activators. This difficulty was resolved in a second series of experiments by using a recombinant $G\alpha_o$ that was uncontaminated by any other Gα subunit. The recombinant was designated $r(+9)\alpha_o$ because it is a fusion polypeptide with nine amino acids added to its natural amino terminus (*13*). This recombinant and other Gα subunits fused in the same way were (i) expressed in *Escherichia coli*, with the use of techniques pioneered by Tabor and Richardson (*14, 15*), (ii) recovered from lysates of the bacteria, (iii) preactivated with GTPγS, and (iv) partially purified by column chromatography (Fig. 2) (*15*).

We tested G_o^* in 66 excised inside-out patches, and positive responses occurred in 34 of them. Of these 34 patches, 15 contain-

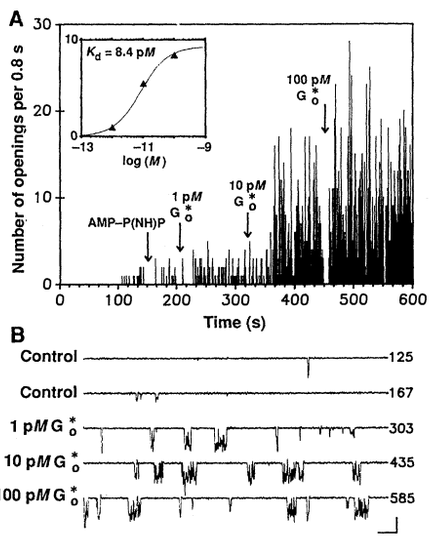

Fig. 1. Brain G_o^* gates single K^+ channel currents in hippocampal pyramidal cells of neonatal rats (*18*) in a concentration-dependent manner. Single K^+ channel currents were recorded from excised inside-out membrane patches (*19–22*). (**A**) The effect of increasing concentrations of G_o^* on a 55-pS K^+ channel (Table 1) is shown by plotting the number of openings per 0.8 s as a function of time for this continuous recording. The nonydrolyzable ATP analog 5′-adenylylimidodiphosphate [AMP-P(NH)P] was added first to inhibit single ATP-sensitive K^+ channel currents that are present in these cells. The inset shows the values averaged for 1 min at each concentration. The points were fitted with the Michaelis relation to give the curve shown. (**B**) Representative traces at different stages of activation. The elapsed time in seconds is indicated to the right of each trace. Holding potential was −80 mV and both bath and pipette solutions contained KMES. Calibrations are 50 ms (*x*) and 3.0 pA (*y*).

A. M. J. VanDongen, R. Joho, A. M. Brown, Department of Physiology and Molecular Biophysics, Baylor College of Medicine, One Baylor Plaza, Houston, TX 77030.
J. Codina, J. Olate, R. Mattera, Department of Cell Biology, Baylor College of Medicine, One Baylor Plaza, Houston, TX 77030.
L. Birnbaumer, Departments of Physiology and Molecular Biophysics and Cell Biology, Baylor College of Medicine, One Baylor Place, Houston, TX 77030.

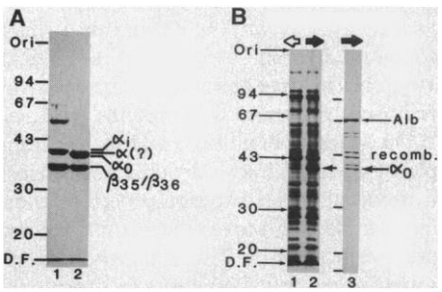

Fig. 2. Patterns produced by bovine brain (**A**) and recombinant (**B**) $G_o\alpha$ subunits after staining 10% SDS-PAGE gels with Coomassie blue (*23*). (A) Lane 1, 3 μg of fraction that eluted before G_o from the DEAE Toyopearl column (referred to as pre-G_o). The most abundant α subunits that were present in this preparation are denoted as α_i and α(?). Lane 2, 3 μg of bovine G_o obtained by DEAE Toyopearl chromatography (*11*). Its principal α subunit is α_o, and it is contaminated by less than 5% of each of the major peptides of the pre-G_o fraction. (B) Lanes 1 and 2, expression in *Escherichia coli* of polypeptides encoded in pT7 α_o plasmid (*15*) as seen on analysis of total bacterial proteins by SDS-polyacrylamide gel. Newly induced recombinant α_o in the total bacterial extract was 8% of total cell protein. Closed arrow, pT7 with the α_o cDNA inserted in the correct, or sense, orientation with respect to the T7 promoter. Open arrow, pT7 with the α_o cDNA inserted in the antisense orientation. Lane 3, GTPγS-activated recombinant α_o after partial purification over DEAE-Sephacel. D.F., dye front; Alb, albumin; Ori, origin.

ing single channels that were stimulated at concentrations of 1 (n = 10) or 10 (n = 5) p*M* were analyzed completely (Table 1). We tested $r(+9)\alpha_o^*$ on 52 patches, and positive responses occurred in 26. Eleven patches, in which $r(+9)\alpha_o^*$ at 14 (n = 6) or 140 (n = 5) p*M* activated K^+ channels, were analyzed completely. These channels fell into the same classes as those activated by G_o^* (Table 1). An example of one response is shown in Fig. 3. Since the effects produced by G_o^* and $r(+9)\alpha_o^*$ were equivalent, the results with both will be treated together.

Simultaneous openings were rare even at the highest concentrations, indicating that there was generally only one channel in each patch responsive to the application of G_o^*. Openings were so infrequent in controls that they could not be characterized, and for all practical purposes G_o^* was obligatory for channel opening (*9*). The G_o-gated channels were not activated by Ca^{2+}, Na^+, or adenosine triphosphate (ATP), since these ligands were absent; unlike serotonin-inhibited K^+ channels (S channels) (*6*), G_o-gated channels were not activated by cytoplasmic second messengers, because the patch was excised. Thus the G_o^*-gated single channel K^+ currents arose from some but probably not all of the K^+ channels coupled by G proteins to neurotransmitter receptors (*1, 2*).

The G_o^*-gated channels could be classified into four types on the basis of slope or chord conductance, open time, and number of openings per burst: 13 pS, 55 pS, and two types of 38-pS channel that differed in kinetics (open time and openings per burst) and inward rectification (Fig. 4 and Table 1). For all classes, the openings occurred in bursts (Figs. 1, 3, and 4 and Table 1) characterized by brief closures within bursts and much longer closures between bursts. With increasing concentrations of G_o^* or $r(+9)\alpha_o^*$, the interburst intervals were shortened but unitary current amplitudes and mean open times were unchanged. Three of the 38-pS channels were demonstrated to conduct only inward currents in symmetrical K^+ solutions (one example is shown in Fig. 4, B and C) and were grouped together with seven other channels that had similar kinetics at −80 mV (Table 1). Three other 38-pS channels, including one with a linear current-voltage (*I-V*) relation (normal rectification), had much longer mean open times at −80 mV and many more openings per burst and were therefore grouped together (Table 1). The open times and number of openings per burst increased with depolarization in the 55-pS and inwardly rectifying 38-pS channels (Fig. 4C). The inwardly rectifying channels may correspond to inwardly rectifying whole-cell K^+ currents that are coupled by G proteins to $GABA_B$, serotonin, and adenosine receptors (*1, 2*). Selectivity for K^+ was demonstrated for three of the 55-pS channels, one of the normally rectifying 38-pS channels, and one of the 13-pS channels because the single channel currents were outward between −40 and 80 mV in asymmetrical K^+-Na^+ solutions. The inwardly rectifying 38-pS channels were probably K^+-selective as well.

In five experiments, prior application of pre-G_o^* at concentrations of 1 to 100 p*M* had no effect, whereas in two experiments, pre-G_o^* activated 13-pS single channel currents. In these instances, G_o^* added subsequently at the same or smaller concentrations produced larger increases in opening probability. The activation could not have been due to GTPγS because the concentrations of GTPγS ($<10^{-10}$ *M*) were the same for G_o^* and pre-G_o^*. Activation of endogenous G protein with GTPγS in the presence of 1 m*M* Mg^{2+} stimulated single channels with currents similar to those stimulated by exogenous G_o^*. Thus, GTPγS at 100 μ*M* stimulated single channels with slope conductances of about 13 (n = 1), 38 (n = 5), and 55 pS (n = 3). These effects, like those produced by G_o^* and $r(+9)\alpha_o^*$, were irreversible during the lifetime (generally 30 min) of the patches.

The G_o^* and endogenous G proteins (activated by GTPγS) had no effect on voltage-dependent transient A channels, which had a conductance of 15 pS, mean open time of 5.0 ms, and 1.5 openings per burst (identified in four patches; tested in two patches). ATP-gated K^+ channels that had a conductance of about 70 pS, a mean open time of 5.0 ms, and about 20 openings per burst were identified in four different patches, and in two cases G_o^* had no effect. Nor did we observe any effects of G_o^* on neuronal voltage-gated Na^+ channels (n = 5).

The $r(+9)\alpha_o^*$ seemed to act specifically, because $r(+9)\alpha_i^*$-1 at higher concentrations (312 p*M*) was ineffective on three $r(+9)\alpha_o^*$-gated 38-pS channels that, on the basis of their kinetics, were inwardly rectifying. A similar sequence occurred for one 38-pS normaly rectifying K^+ channel with $r(+9)\alpha_i^*$-2 at 180 p*M* and for one 13-pS channel with $r(+9)\alpha_s^*$ (279 amino acids) at 90 p*M*. However, we cannot exclude the possibility that $G_i\alpha s$ may in some cases also activate $G_o\alpha$-gated channels. The potency of the $r(+9)\alpha_o^*$ was about one-fifteenth that of brain G_o^*, which at 1 to 10 p*M* had similar effects (Fig. 1A). Reductions in potency have been described for the effects of recombinant bacterial α_s^* on adenylyl cyclase (*13, 16*) and Ca^{2+} channels (*13*) and for the effects of recombinant bacterial α_k^* on K^+ channels (*13*). These reductions in potency

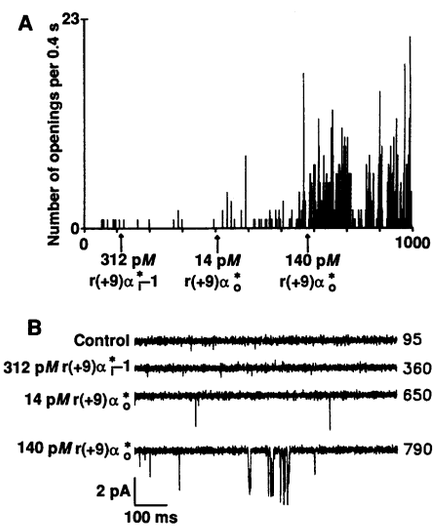

Fig. 3. Effects of recombinant bacterial Gα subunits on a neonatal rat hippocampal pyramidal cell K^+ channel. Single channel currents from a 38-pS K^+ channel were recorded in symmetrical KMES solutions at −80 mV. Top record (**A**) is a diary of the experimental run showing the number of openings per 0.4 s as a function of time. Below (**B**) are faster time base records showing single channel K^+ currents. The numbers to the right in (B) correspond to the elapsed time in seconds in (A). Preactivated recombinant α_i-1 [$r(+9)\alpha_i^*$-1] had no effect, whereas preactivated recombinant α_o [$r(+9)\alpha_o^*$] produced a concentration-dependent stimulation of these currents.

were similar for fusion and nonfusion recombinant α_s^*s (*13*) and were associated with equivalent reductions in affinity for both effectors without changes in stimulatory capacity (*13, 16*). Both recombinants interacted with β-adrenergic receptors, βγ dimers, and guanine nucleotides normally and retained their relative effector specificities. Hence, the recombinant experiments, despite the limitation of reduced potency, establish $G_o\alpha$ as a specific Gα activator of brain K^+ channels.

Brain G_o activated four different members of the family of brain K^+ channels, although many others were not stimulated, such as Ca^{2+}-activated channels, A channels (*5*), delayed rectifier channels (*5*), S channels (*4*), and ATP-gated channels. The activation by G_o was membrane-delimited and may have been direct; any intervening membrane protein would have acted independently of Ca^{2+}, Mg^{2+}, ATP, or guanosine triphosphate (GTP) and would have been intimately associated with four different types of K^+ channels. Other qualifications include (i) some G_o^*-activated single channel currents, recorded at −80 mV in isotonic K^+ solutions, could have arisen from nonselective cation channels; (ii) the amplitude probability density functions had shoulders (Fig. 4, A and B) that resulted from subconductance states that have not been analyzed further; (iii) cytoplasmic mediators were absent, and these could modify the action of G_o^* in intact cells; and (iv) the neurotransmitter receptors that are coupled to these G_o-gated channels have not been determined. However, the identity of one of the receptors was inferred from cell-attached recordings before patch excision. With the patch pipette containing serotonin at 1 to 10 μ*M* (*n* = 15), single channel currents were plentiful and identification of predominant types was difficult, although inwardly rectifying 38-pS channels were identified. After excision into GTP-free bathing solution, ligand-gated activity became sparse but was reconstituted by the addition of GTPγS at 100 μ*M* (*n* = 2).

Whole-cell current experiments have shown that G_o at nanomolar concentrations can reconstitute receptor interactions with Ca^{2+} channels in neuron-like cells such as neuroblastoma-glioma hybrid cells (*5*) or dorsal root ganglion cells (*5*). However, in no case was the specificity of $G_o\alpha$ over other Gαs determined definitely; this is important because picomolar concentrations were effective in the present experiments. Nor was the participation of second messengers excluded; in fact, the inhibition of Ca^{2+} currents can be mimicked by protein kinase C activating phorbol esters (*17*). In contrast, we could identify distinct brain K^+ channels, specify a particular $G_o\alpha$-subunit activator of these K^+ channels, and exclude the participation of cytoplasmic second messengers. We conclude that a principal function of G_o in signal transduction in the brain is to couple neurotransmitter receptors to K^+ channels within the plasma membrane of brain cells.

Table 1. Conductance and kinetics of G_o-gated brain single channel K^+ currents. Four classes of K^+ channels that were gated by brain G_o^* or $r(+9)\alpha_o^*$ were identified by their conductance and kinetics.

Activated by		Conductance in pS (mean ± SD)	Open time in ms (mean ± SD)	Openings per burst (mean ± SD)
G_o^*	$r(+9)\alpha_o^*$			
6	1	54.5 ± 3.6	2.76 ± 1.22	5.05 ± 3.34
5	5	37.5 ± 2.6	1.60 ± 0.42	1.61 ± 0.29
2	1	37.5 ± 1.7	4.59 ± 0.99	4.39 ± 0.31
2	4	12.7 ± 2.5	2.30 ± 1.70	1.54 ± 0.29

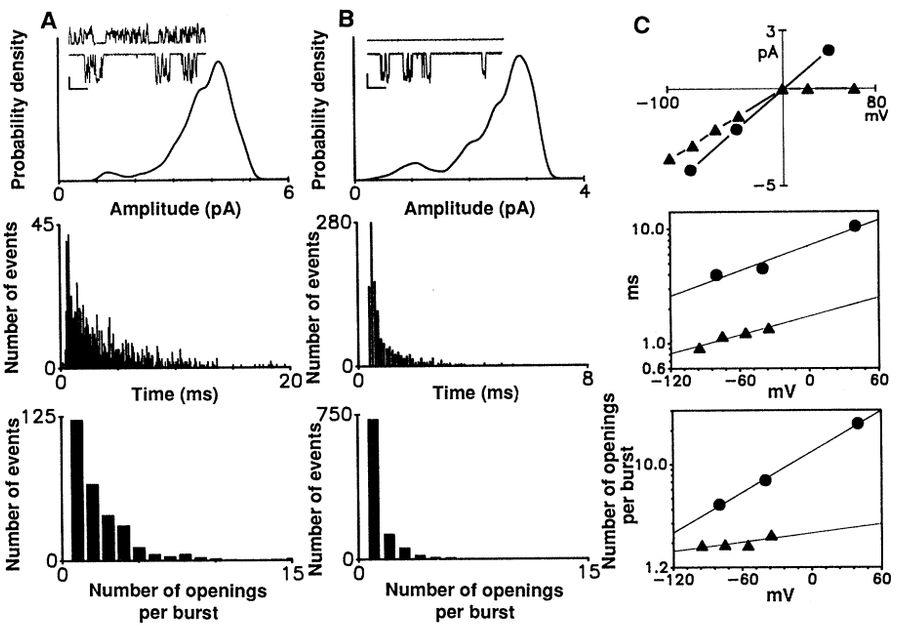

Fig. 4. Properties of the two major classes of G_o-gated, single channel K^+ currents from hippocampal pyramidal cells; these are the 55-pS (**A**) and the 38-pS inwardly rectifying classes (**B**). The holding potential was −80 mV except where otherwise specified, and the solutions were symmetrical isotonic K^+ solutions. The insets in row 1 of columns A and B show the currents at +40 (above) and −80 (below) mV. Calibrations were 2 pA and 20 ms. The amplitude probability densities (top row columns A and B) were estimated with a kernel method (*24*). The modus, the current with the maximum probability density, was used as an estimate for the single channel current amplitude. The open time histograms are shown in the second row of A and B and the mean open times were 3.96 and 1.84 ms, respectively. The third row of A and B shows the frequency distributions of the number of openings per burst. A burst is defined as consecutive openings separated by closed times shorter than 5 ms. This critical closed time was chosen arbitrarily and was fixed for all single channel currents analyzed. The mean numbers of openings per burst were 4.4 and 1.9 for A and B, respectively. The top panel of column **C** shows the single channel *I-V* relations for a normally rectifying 55-pS channel and an inwardly rectifying 38-pS channel. The voltage dependence of the open times and numbers of openings per burst are shown in the middle and bottom panels. Filled circles represent the 55-pS channel, and filled triangles represent the 38-pS channel.

REFERENCES AND NOTES

1. R. A. Nicoll, *Science* **241**, 545 (1988).
2. R. A. North, J. T. Williams, A. Surprenant, M. J. Christie, *Proc. Natl. Acad. Sci. U.S.A.* **84**, 5487 (1987); S. Mihara, R. A. North, A. Surprenant, *J. Physiol. (London)* **390**, 335 (1987); R. Andrade, R. C. Malenka, R. A. Nicoll, *Science* **234**, 1261 (1986); L. O. Trussell, and M. B. Jackson, *J. Neurosci.* **7**, 3306 (1987); B. H. Gähwiler and D. A. Brown, *Proc. Natl. Acad. Sci. U.S.A.* **82**, 1558 (1985); K. Sasaki and M. Sato, *Nature* **325**, 259 (1987); Y. Nakajima, S. Nakajima, M. Inoue, *Proc. Natl. Acad. Sci. U.S.A.* **85**, 3643 (1988); G. K. Aghajanian and Y.-Y. Wang, *Brain Res.* **371**, 390 (1986); R. A. North and J. T. Williams, *J. Physiol. (London)* **364**, 265 (1985); J. L. Yakel, L. O. Trussell, M. B. Jackson, *J. Neurosci.* **8**, 1273 (1988); S. D. Moore, S. G. Madamba, M. Joëls, G. R. Siggins, *Science* **239**, 278 (1988); R. H. Thalmann, D. Grenet, L. Birnbaumer, *Soc. Neurosci. Abstr.* **13**, 1005 (1988).
3. P. C. Sternweis and J. D. Robishaw, *J. Biol. Chem.* **259**, 13806 (1984); R. M. Huff, J. M. Axton, E. J. Neer, *ibid.* **260**, 10864 (1985); P. Gierschik *et al.*, *Proc. Natl. Acad. Sci. U.S.A.* **83**, 2258 (1986); P. F. Worley *et al.*, *ibid.*, p. 4561; A. G. Gilman, *Annu. Rev. Biochem.* **56**, 615 (1987); P. Brabet *et al.*, *J. Neurosci.* **8**, 701 (1988).
4. H. Itoh *et al.*, *Proc. Natl. Acad. Sci. U.S.A.* **83**, 3776 (1986).
5. G. G. Holz IV, S. G. Rane, K. Dunlap, *Nature* **319**,

670 (1986); K. Dunlap, G. G. Holz IV, S. G. Rane, *Trends Neurosci.* **10**, 241 (1987); R. H. Scott and A. C. Dolphin, *J. Physiol. (London)* **386**, 1 (1987); *Nature* **320**, 760 (1987); E. Wanke *et al.*, *Proc. Natl. Acad. Sci. U.S.A.* **84**, 4313 (1987); J. Hescheler, W. Rosenthal, W. Trautwein, G. Schultz, *Nature* **325**, 445 (1987); D. A. Ewald, P. C. Sternweis, R. J. Miller, *Proc. Natl. Acad. Sci. U.S.A.* **85**, 3633 (1988); R. M. Harris-Warrick *et al.*, *Neuron* **1**, 27 (1988).

6. M. J. Schuster, J. S. Camardo, S. A. Siegelbaum, E. R. Kandel, *Nature* **313**, 392 (1985); D. Piomelli *et al.*, *ibid.* **328**, 38 (1987); S. A. Siegelbaum, J. S. Camardo, E. R. Kandel, *ibid.* **299**, 413 (1982).
7. M. Rogawski, *J. Neurophysiol.* **56**, 481 (1986); M. Simonneau, C. Distasi, L. Tauc, G. Barbin, *Brain Res.* **412**, 224 (1987).
8. C. K. Sole, W. N. Zagotta, R. W. Aldrich, *Science* **236**, 1094 (1987); L. S. Liebovitch and J. M. Sullivan, *Biophys. J.* **52**, 979 (1987).
9. A. M. Brown *et al.*, *Cold Spring Harbor Symp. Quant. Biol.*, in press; A. Yatani, J. Codina, A. M. Brown, L. Birnbaumer, *Science* **235**, 207 (1987); J. Codina, A. Yatani, D. Grenet, A. M. Brown, L. Birnbaumer, *ibid.* **236**, 442 (1987); G. Kirsch, A. Yatani, J. Codina, L. Birnbaumer, A. M. Brown, *Am. J. Physiol.*, in press; A. Yatani, J. Codina, R. D. Sekura, L. Birnbaumer, A. M. Brown, *Mol. Endocrinol.* **1**, 283 (1987); J. Codina, D. Grenet, A. Yatani, L. Birnbaumer, A. M. Brown, *FEBS Lett.* **216**, 104 (1987); A. Yatani *et al.*, *J. Biol. Chem.*, in press; A. Yatani *et al.*, *Science* **238**, 1288 (1987); Y. Imoto *et al.*, *Am. J. Physiol.*, in press.
10. T. Katada, M. Oinuma, M. Ui, *J. Biol. Chem.* **261**, 8182 (1986).
11. Bovine brain G_o was purified by a procedure for homogenization of membrane preparations [E. J. Neer, J. M. Lok, L. G. Wolf, *J. Biol. Chem.* **259**, 14222 (1984)] and procedures of extraction and chromatography [J. Codina *et al.*, *ibid.*, p. 5871; J. Codina, W. Rosenthal, J. D. Hildebrandt, R. D. Sekura, L. Birnbaumer, *J. Receptor Res.* **4**, 411 (1984)]. The basic buffer system was 1 m*M* EDTA, 20 m*M* β-mercaptoethanol, 10 m*M* Na Hepes, *p*H 8.0, and 30% (v/v) ethyleneglycol (buffer A). The chromatography steps for human erythrocyte G proteins included: (i) DEAE-Sephacel chromatography (5- by 60-cm bed volume, NaCl gradient; buffer A with 0.9% cholate), (ii) a sizing step over AcA-34 Ultrogel (5- by 60-cm bed volume), (iii) heptylamine-Sepharose chromatography (5 by 60 cm; positive cholate gradient as described for chromatography of the Ultrogel peak A of human erythrocyte G_s activity), (iv) and second (cholate gradient; buffer A with 0.5% Lubrol PX) and third DEAE-Sephacel (NaCl gradient; buffer A with 0.5% Lubrol PX) chromatographies. This resulted in a mixture of G proteins referred to as "G_i/G_o," made up of approximately 15% G_{41} (migration on SDS-polyacrylamide gel with approximate molecular mass of 41,000 daltons; also known as brain G_i, 75% G_o (migration on SDS-polyacrylamide gel with an approximate molecular mass of 39,000 daltons), and about 5% other components. One of these components, which migrated at about 55,000 daltons, predominated and was insenstivie to PTX. Of two other components that migrated between G_i and G_o, one was PTX-sensitive [possibly G_{40} (T. Katada, M. Oinuma, K. Kusakabe, M. Ui, *FEBS Lett.* **353**, 213 (1987)] and the other was PTX-insensitive. The latter is barely noticeable on staining with Coomassie blue but is distinct on staining with silver. G_i/G_o was fractionated further by DEAE-Toyopearl chromatography (1 by 10 cm, buffer A with 0.6% Lubrol PX, 0 to 400 m*M* NaCl gradient), yielding two fractions: (i) highly enriched G_o, essentially free of the G_{41} and G_{40} PTX substrates and the 55,000-dalton material but containing perhaps as much as 5% of a PTX-insensitive material migrating close to G_o; and (ii) a pool of proteins that eluted before G_o. This pool was called pre-G_o and was composed of 50 to 60% of the G_{41} PTX substrate (Fig. 2A, lane 1, α_i), 20 to 30% of a G_{40}-like PTX substrate (Fig. 2A, lane 1, α?), and up to 20% of the 55,000-dalton contaminant. Less well-defined bands of PTX substrates eluted after the G_o peak and were not tested. The Coomassie blue stain of pre-G_o and G_o as seen with SDS-polyacrylamide gel is shown in Fig. 2. G_o and pre-G_o were concentrated to 100 to 120 μg/ml by free-flow electrophoresis [M. W. Hunkapillar, E. Lujan, F. Ostrander, L. E. Hood, *Methods Enzymol.* **91**, 227 (1983)] into buffer A with 0.1% Lubrol PX and 100 μ*M* GTP and activated at 50 to 100 μg/ml in buffer A with 0.1% Lubrol PX, 50 m*M* $MgCl_2$, and 1 μ*M* [^{35}S]GTPγS (150 cpm/pmol) by incubation for 30 min at 32°C. This was followed by extensive dialysis against buffer A containing 50 m*M* $MgCl_2$, 20 m*M* KCl, and 0.1% Lubrol PX until the total concentration of [^{35}S]GTPγS was reduced to less than 2 μ*M* as assessed by liquid scintillation spectroscopy. The G_o^* and pre-G_o^* were stored as α-GTPγS plus βγ mixtures at −70°C until used. Prior to use, the activated proteins were diluted with bathing buffer to give the final concentrations indicated in the text and figures.
12. H. Fong, K. Yoshimoto, P. Eversole-Cire, M. Simon, *Proc. Natl. Acad. Sci. U.S.A.* **85**, 3066 (1988).
13. R. Mattera *et al.*, *J. Biol. Chem.*, in press; L. Birnbaumer *et al.*, *Cold Spring Harbor Symp. Quant. Biol.*, in press; R. Mattera *et al.*, in preparation.
14. S. Tabor, dissertation, Harvard University (1987); S. Tabor and C. C. Richardson, *Proc. Natl. Acad. Sci. U.S.A.* **82**, 1074 (1985); S. Tabor, H. E. Huber, C. C. Richardson, *J. Biol. Chem.* **262**, 16212 (1987).
15. The expression plasmid for bacterial synthesis of recombinant α_o was constructed as follows. A rat heart α_o cDNA of 1302 nucleotides (nt), beginning with nt 3 of the open reading frame (ORF) and extending 237 nt beyond the TGA stop codon and having a nucleotide composition identical to that published for rat olfactory epithelial α_o by D. T. Jones and R. R. Reed [*J. Biol. Chem.* **262**, 14241 (1987)], was cloned from a λ gt11 cDNA library constructed from rat heart polyadenylated mRNA with an oligonucleotide complementary to the coding strand of rat brain α_o that encodes amino acids 70 to 85 (*4*). Assigning number 1 to nt A of the ATG initiation codon of the cDNA, the following modifications and fragment transfers were made. The insert was excised with Eco RI and subcloned into the Eco RI site of M13mp19 [T. Maniatis, E. F. Fritsch, J. Sambrook, *Molecular Cloning: A Laboratory Manual* (Cold Spring Harbor Laboratory, Cold Spring Harbor, NY, 1982)]. The coding sequence was completed by insertion of AT at the 5′ end, thus creating a C′CATGG Nco I site, and by the removal of the internal Nco I site at 260 to 265 by replacing C 261 with nt A. For oligonucleotide-directed replacements and insertions [J. W. Taylor, J. Ott, F. Eckstein, *Nucleic Acids Res.* **13**, 8764 (1985)], we used reagents and protocols obtained in kit form from Amersham, and oligonucleotides were synthesized on a Du Pont Coder 300 apparatus. Modifications were confirmed by sequencing with the dideoxynucleotide chain termination method [F. Sanger, S. Nicklen, A. B. Coulson, *Proc. Natl. Acad. Sci. U.S.A.* **74**, 5463 (1977)]. The 1306-nt Nco I/Eco RI fragment (formed of the −1 to 1303 rat heart α_o cDNA containing a 237-nt 3′ untranslated region ending with 13 A's) was excised, filled with Klenow fragment of DNA polymerase, and subcloned by blunt-end ligation into the also filled Bam HI site of the polylinker of the pT7-7 vector, giving the pT7-α_o expression plasmid. Part of the nucleotide composition of the 5′ region that flanks the ORF of the α_o subunit is:

```
nt   -41  -36        -27     -21                      -1 1
       AAGGAG ATATACAT ATG GCT AGA ATT CGC GCC CGG GGA TCC ATG of α_o subunit
ORF      rbs            Met Ala Arg Ile Arg Ala Arg Gly Ser Met
         aa              -1  -2  -3  -4  -5  -6  -7  -8  -9   1
```

where nt −41 to −21 are pT7 gene-10 sequences including the ribosomal binding site (*rbs*: nt −41 to −36), the two first codons and the first nucleotide of the third codon of the gene 10 ORF (nt −27 to −21), and nt −20 to −1 are what remains of the cloning cassette of pT7-7. The recombinant was expressed in transformed *E. coli* K38 cells (*13*). Cells from 42 ml of culture, pulsed during the last 10 min of induction with 1 mCi/ml [^{35}S]methionine, were pelleted at 0° to 4°C and lysed [E. Seeburg, J. Nissen-Meyer, P. Strike, *Nature* **263**, 524 (1976)]. After lysis, 0.02 volumes of 100 m*M* diisopropylfluorophosphate (DIFP) in propyleneglycol were added and then 20 μ*M* GTPγS, 8 m*M* $MgCl_2$, 1 m*M* EDTA, 20 m*M* β-mercaptoethanol, 20 m*M* tris-HCl, *p*H 8.0, and 30% (v/v) ethyleneglycol. The recombinant α_o was activated by incubation for 30 min at 32°C. The mixture was centrifuged for 30 min at 30,000*g* and 4°C. The supernatant was diluted by a factor of five with 20 m*M* β-mercaptoethanol, 5 m*M* $MgCl_2$, 1 m*M* EDTA, 15 m*M* tris-HCl, *p*H 8.0, and 30% ethyleneglycol and the mixture was applied to a DEAE-Sephacel column (height 9 cm; diameter 1 cm) equilibrated with buffer at 0° to 4°C. The column was washed with five volumes of buffer, then eluted with a linear gradient from 0 to 500 m*M* NaCl in the same buffer. Fractions of 1 ml were collected and analyzed for protein content by SDS-polyacrylamide gel, followed by Coomassie blue staining and autoradiography, the latter to locate the newly synthesized α subunit. Under these conditions, the recombinant α_o subunit (fractions 20 to 25) was pooled, mixed with [^{35}S]GTPγS to give 100,000 cpm/μl, and placed on top of Centricon 10 microconcentrators (Amicon) and concentrated between 15- and 25-fold. The concentrates were diluted with buffer lacking ethyleneglycol and reconcentrated five times. This resulted in removal of at least 99.99% of the added free GTPγS to a maximal concentration of no more than 3 n*M*. A further dilution by at least 5×10^5 occurred during the experiment. In the experiment in Fig. 4, the concentration of GTPγS-activated recombinant α_o subunit (Fig. 2B, lane 3, recombinant α_o^*) in the pooled and concentrated fractions was estimated to be 700 n*M* by quantitative densitometry.
16. M. P. Graziano, P. J. Casey, A. G. Gilman, *J. Biol. Chem.* **262**, 11375 (1987); M. P. Graziano, M. Freissmuth, A. G. Gilman, *J. Biol. Chem.*, in press; R. Mattera *et al.*, *Science*, in press.
17. S. G. Rane and K. Dunlap, *Proc. Natl. Acad. Sci. U.S.A.* **83**, 184 (1986); C. Marchetti and A. M. Brown, *Am. J. Physiol.* **254**, C206 (1988); A. E. Lacerda, D. Rampe, A. M. Brown, *Nature* **335**, 249 (1988).
18. Primary cultures of rat hippocampal pyramidal cells were prepared with methods modified from J. E. Huettner and R. W. Baughman [*J. Neurosci.* **6**, 3044 (1986)]. Tissue from hippocampal CA1 regions was obtained by microdissection from newborn (1- to 2-day-old) Wistar rats, dissociated by gentle trituration after enzyme treatment, and plated on collagen–poly-D-lysine–coated cover slips. Cells were maintained in culture for up to 4 weeks in a medium containing minimum essential medium with Earle's salts (Gibco Laboratories), 5% fetal bovine serum, and serum extender (Collaborative Research).
19. Single channel currents were recorded from inside-out membrane patches excised from the somas of large neurons after formation of a gigaohmseal (*22*). An EPC7 (List Electronics) was used as the patch clamp amplifier. Pipettes were pulled from TW150F glass tubing and were coated with Sylgard. Pipette resistance after filling ranged from 10 to 20 megohms in the bath.
20. The substrate-free bath solution contained 130 m*M* potassium methane sulfate, 1 m*M* $MgCl_2$, 5 m*M* EGTA, 10 m*M* Hepes, and tris to adjust *p*H to 7.4. This solution is referred to as KMES. The pipette contained either this solution or an equimolar substitution of sodium methane sulfate for potassium methyl sulfate. AMP-P(NH)P was added to the bath, either before or after excision, at a final concentration of 200 μ*M*. All experiments were done at room temperature (21° ± 1°C). The recording chamber was coated with bovine serum albumin to prevent the G proteins from sticking to the glass bottom. The Ag-AgCl ground electrode was connected to the bath with a disposable agar bridge, which was replaced after each patch. Activated G proteins were diluted in KMES from a stock solution of 100 n*M*. The bath had a volume of 500 μl, and G proteins were applied to the bath in a volume of 50 μl to obtain good mixing.
21. Continuous recordings were digitized (14-bit A-D converter) and stored on disk with a capture algorithm (*22*). The analysis was done on a microVax II

(Digital Equipment Corporation), with custom-made analysis software. Typically, the sampling rate was 10 kHz and signals were filtered at 1.5 kHz (48 dB/octave, Bessel characteristic). Single channel openings were detected and idealized by an algorithm that used both amplitude and slope information. The amplitude of the openings and the duration of both openings and closures were stored for subsequent statistical analysis.
22. O. P. Hamill, A. Marty, E. Neher, B. Sakmann, F. Sigworth, *Pflüegers Arch.* **391**, 85 (1981); D. Colquhuon and F. J. Sigworth, in *Single-Channel Recording*, E. Neher and B. Sakmann, Eds. (Plenum, New York, 1983), pp. 191–263.
23. U. Laemmli, *Nature* **227**, 680 (1970).
24. B. W. Silverman, *Density Estimation* (Chapman & Hall, New York, 1986).
25. Supported in part by NIH grants HL-31154 and DK-19318 to L.B., and NIH grants HL-37044 and HL-36930 to A.M.B. We thank G. Schuster for help with dissection and culturing of hippocampal pyramidal cells. We thank J. Breedlove, G. May, and D. Witham for their secretarial assistance.

12 July 1988; accepted 4 October 1988

Experimentally Induced Visual Projections into Auditory Thalamus and Cortex

MRIGANKA SUR,* PRESTON E. GARRAGHTY, ANNA W. ROE

Retinal cells have been induced to project into the medial geniculate nucleus, the principal auditory thalamic nucleus, in newborn ferrets by reduction of targets of retinal axons in one hemisphere and creation of alternative terminal space for these fibers in the auditory thalamus. Many cells in the medial geniculate nucleus are then visually driven, have large receptive fields, and receive input from retinal ganglion cells with small somata and slow conduction velocities. Visual cells with long conduction latencies and large contralateral receptive fields can also be recorded in primary auditory cortex. Some visual cells in auditory cortex are direction selective or have oriented receptive fields that resemble those of complex cells in primary visual cortex. Thus, functional visual projections can be routed into nonvisual structures in higher mammals, suggesting that the modality of a sensory thalamic nucleus or cortical area may be specified by its inputs during development.

WHAT IS INTRINSICALLY "VISUAL" about visual thalamus and cortex? Can visual projections be induced into nonvisual targets, and are these projections functional? The organization of the visual pathway in ferrets is similar to that in cats (*1*); the visual system of cats has been studied extensively both anatomically and physiologically. However, unlike cats, retinofugal projections in ferrets are very immature at birth (*2*); we reasoned that it might be possible to induce extensive plasticity in the retinothalamic pathway by surgery in neonatal ferrets.

Retinal targets were reduced in newborn ferret pups by ablating the superior colliculus and visual cortical areas 17 and 18 of one hemisphere (*3*) (Fig. 1). Ablating visual cortex causes the lateral geniculate nucleus (LGN) in the ipsilateral hemisphere to atrophy severely by retrograde degeneration. Concurrently, alternative target space for retinal afferents was created in the medial geniculate nucleus (MGN) by either ablating the inferior colliculus or sectioning fibers ascending to the MGN in the brachium of the inferior colliculus (*4, 5*).

Department of Brain and Cognitive Sciences, Massachusetts Institute of Technology, Cambridge, MA 02139.

*To whom correspondence should be addressed.

Experiments were done on 10 normal adult ferrets and 16 operated ferrets that were reared to adulthood. In five operated animals, intravitreal injections of anterograde tracers (*6*) revealed retinal projections to normal thalamic targets, including the surviving, shrunken LGN, as well as aberrant projections to auditory thalamic nuclei (Fig. 2). The new retinal projection zones included patches of the dorsal, medial, and ventral (or principal) divisions of the MGN, as well as parts of the lateral posterior nucleus and the posterior nuclear complex adjacent to the MGN. The retinal projections to the MGN complex occupied up to one-third of the volume of the MGN. We confirmed that the MGN in operated animals projected normally to auditory cortex (Fig. 1), both by the transneuronal label in auditory cortex after intraocular injections (*6*) and by the extensive retrograde labeling of cells in the MGN after restricted injections of horseradish peroxidase (HRP) or fluorescent retrograde tracers into primary auditory cortex (Fig. 2).

These experiments also indicated that the ipsilateral MGN is the major route for visual inputs to reach primary auditory cortex. Along with receiving major thalamic projections from the various divisions of the MGN (*7*), the primary auditory cortex in operated animals retained its connections with other auditory cortical areas. These included ipsilateral and contralateral connections with the second auditory area located lateral to primary auditory cortex and with areas on the ectosylvian gyrus located anterior, posterior, and ventral posterior to primary auditory cortex (*8*).

We next recorded responses of cells electrophysiologically from the MGN in operated animals (*9*) and compared visual responses there with responses from the surviving LGN in the same animals as well as from the LGN in normal animals. We studied the visual responses of single cells to various tests (*10*). We also tested the auditory responses of cells in the auditory thalamus with click or tone stimuli delivered through earphones.

In the LGN of normal animals, we recorded X, Y, and W cells (Fig. 3A); X and Y cells were found in the A laminae, and Y and

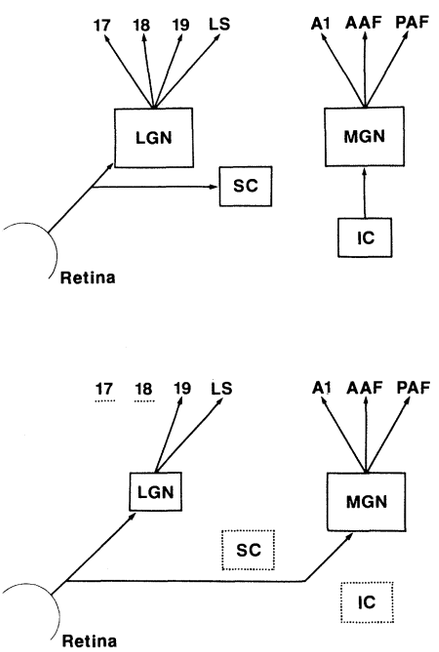

Fig. 1. The experimental design for induction of visual projections to the auditory system in ferrets. (**Top**) Projections in normal animals. The retina projects to LGN and superior colliculus (SC). The LGN projects to cortical areas 17 (primary visual cortex or striate cortex) and 18 as well as to other extrastriate areas including area 19 and the lateral suprasylvian (LS) cortex. In the auditory system, the inferior colliculus (IC) projects to the MGN. The ventral and the dorsal division of the MGN project heavily to primary auditory cortex (A1), as well as to other cortical areas including the anterior auditory field (AAF) and the posterior auditory field (PAF) in cortex (*29*). (**Bottom**) If cortical areas 17 and 18 are ablated in neonatal ferrets, the LGN atrophies severely by retrograde degeneration. Ablating the superior colliculus as well, and deafferenting the MGN by ablating the inferior colliculus or sectioning fibers ascending from it, causes the retina to project to the MGN and hence to auditory cortex.